scientific reports

OPEN

Insights into the interaction of Fibrinogen with Timolol Maleate and elucidation of binding sites via. spectroscopic and molecular docking study

Neha Govind Rao[1], Anu Radha Pathania[1], Harman Deep Kour[1], Suhas Ballal[2], Abhayveer Singh[3], Abhijit Bhowmik[4,5] & Balewgize Amare Zeru[6✉]

Timolol maleate (TM), a beta-blocker drug, is used in treating conditions related to arterial hypertension. Exploring the possible interaction between TM and plasma proteins is crucial for enhancing the drug potency. This interaction study is done to examine the impact of TM on the comportment of bovine plasma Fibrinogen (FB) by utilizing spectroscopic and computational techniques such as fluorescence spectroscopy, circular dichroism (CD), and molecular docking. Employing fluorescence spectroscopy at temperatures 290 K, 298 K, and 308 K disclosed that TM used hydrophobic interactions to quench the intrinsic fluorescence of FB and show a hypochromic shift. The values of the binding and quenching rate constant specify the strong interaction between the TM and FB. The thermodynamic parameters such as ΔH and ΔG unveil the existence of hydrophobic forces. The CD demonstrates the influence of TM on the secondary structure of FB. Molecular docking revealed the theoretical evaluation of FB and TM binding. The investigation provides insightful information on stability, pharmacokinetics and bioavailability of TM, which is crucial for maximizing its therapeutic value.

Keywords Circular dichroism, Fibrinogen, Fluorescence spectroscopy, Molecular Docking, Timolol maleate

Abbreviations
FB   Fibrinogen
TM   Timolol Maleate
CD   Circular Dichroism

The large size and complicated structure characterize the complex fibrous glycoprotein Fibrinogen (FB), which consists of three pairs of polypeptide chains held together by 29 disulfide links. Alpha-helical coiled coil rods connect the globular domains at both extremities and the center, spanning 45 nm in length[1-5]. FB is found in blood at a concentration of 1.5–4.0 g/L and is the third major plasma protein after immunoglobulin and serum albumin. Fibrinogen is a soluble glycoprotein arranged in a dimer that has been extensively studied for its role in blood clotting. Aα, Bβ, and γ chains in humans are commonly found to have 610, 461, and 411 amino acids, respectively. Researchers have studied the geometry of FB and its organization into domains or independently folded components using a variety of physicochemical and structural techniques. This glycoprotein is vital for various biological processes, including haemostasis, inflammation, wound healing, and angiogenesis. Studies

[1]Department of Chemistry, University Institute of Sciences, Chandigarh University, Gharuan, Mohali 140413, Punjab, India. [2]Department of Chemistry and Biochemistry, School of Sciences, JAIN (Deemed to be University), Bangalore, Karnataka, India. [3]Centre for Research Impact & Outcome, Chitkara University Institute of Engineering and Technology, Chitkara University, Rajpura 140401, Punjab, India. [4]Department of Additive Manufacturing, Mechanical Engineering, SIMATS, Saveetha Institute of Medical and Technical Sciences, Thandalam, Chennai 602105, India. [5]Division of Research and Development, Lovely Professional University, Punjab, Phagwara, India. [6]Faculty of Mechanical Engineering, Jimma Institute of Technology, Jimma University, Jimma, Ethiopia. ✉email: balewgize.zeru@ju.edu.et

have revealed FB's significant role in cellular migration, wound organization, and the enhancement of wound strength and stability throughout the healing process[5–10].

In the realm of traditional pharmacology, beta blockers function as antagonists to beta-adrenergic receptors, which play a vital role in regulating numerous physiological processes, including metabolic functions, central nervous system activities, blood pressure, heart rate, and airway responsiveness[11–13]. These medications are typically classified into two main groups: selective and non-selective beta-blockers. Timolol maleate (TM) exemplifies a non-selective beta-blocker, with the chemical composition [(4-morpholino-1,2,5-thiadiazol-3-yl) oxy]-1-(tert-Butyl-amino)-3- [1-to-2-propanol maleate (salt) ratio. This compound has a molecular weight of 432.49 g/mol and is represented by the chemical formula $C_{13}H_{24}N_4O_3S·C_4H_4O_4$. While insoluble in ether and cyclohexane, TM readily dissolves in water, alcohol, and methanol. It exhibits limited solubility in propylene glycol and chloroform and melts within the range of 202–203 °C[14–16]. TM affects both beta 1 and beta 2 (beta-adrenergic receptors) without significant direct intrinsic sympathomimetic, myocardial depressive, or local anaesthetic effects. Its effectiveness in reducing intraocular pressure makes it a common prescription for patients with open-angle and aphakic glaucoma. Additionally, TM is utilized in the management of hypertension and for reducing cardiovascular mortality and reinfarction risk in clinically stable patients who have survived the acute phase of myocardial infarction[17,18]. Figure 1 demonstrates the molecular structure of TM.

Drug-plasma protein binding provides crucial insights into a drug's pharmacokinetic and pharmacodynamic characteristics, as well as its distribution patterns. The binding phenomenon of TM and FB may result in considerable alteration in the apparent volume of distribution and hepatic and renal clearance; thus, the free-to-total drug ratio in plasma alters without affecting the pharmacodynamics[19]. Studies on protein-drug interactions are very significant in clarifying the molecular mechanism involved in medication potency, target selectivity, and side effects. Several interactions include the binding of medicinal substances to specific binding sites of proteins that alter many biological activities and protein structures, which helps researchers predict the off-target effects of medicines and improves the bioavailability of drugs and their efficacy[20,21]. To determine if FB acts as an off-target binding partner for TM, which might lead to changes in drug distribution or abrupt biological ramifications, such as amplification of coagulation processes. We used circular dichroism (CD), fluorescence, and molecular docking as experimental techniques that provide insight into the binding mechanism of TM and FB, which is important for assessing TM's interaction in intricate biological systems[22–24]. This research is crucial not only for enhancing drug efficacy but also for filling a fundamental knowledge gap regarding how TM interacts with plasma proteins, particularly FB and how such interactions affect drug pharmacokinetics, bioavailability and efficacy. Fibrinogen, an important constituent of the coagulation system, is not only extremely prevalent in circulation but also plays a major role in drug binding, stability and possible side effects. Justifying this emphasis, investigation of TM-FB interactions offers novel insights into drug behaviour in physiological environments, which can be utilized for the optimization of drug formulations, reducing adverse effects, improving targeted drug delivery and enhancing therapeutic outcomes.

Methods
Materials
Fibrinogen from bovine plasma- 65–85% protein (≥75%, Sigma–Aldrich) and Timolol maleate were acquired from Sigma–Aldrich Chemical Co. The study utilized exclusively analytical-grade reagents, along with deionized water throughout. Stock solutions of TM and FB were prepared by dissolving precise quantities of each solid powder in an aqueous phosphate buffer solution. The phosphate buffer (0.05 M, pH 8.4) was created by combining sodium dihydrogen orthophosphate and disodium hydrogen orthophosphate with double deionized water to the appropriate concentration, followed by homogenization for subsequent analysis.
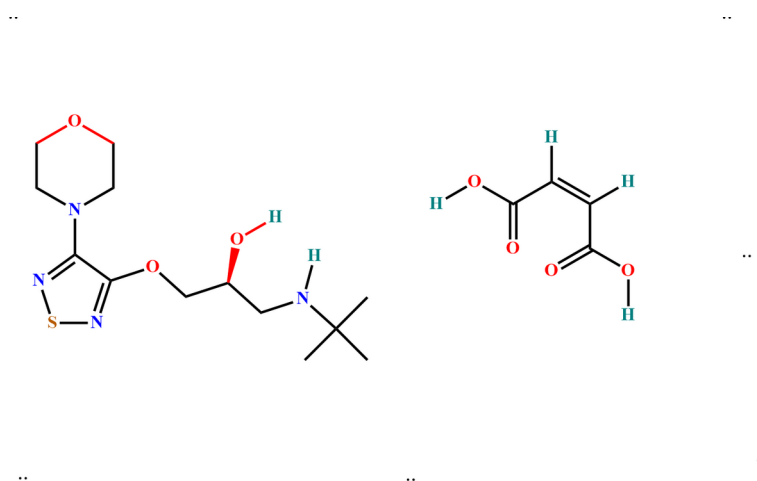

Fig. 1. Structural visualization of Timolol Maleate.

Methodology

Fluorescence spectroscopy
A Shimadzu 5301PC fluorescence spectrophotometer, featuring a xenon lamp and 10 nm spectral width, was employed to measure fluorescence intensity. The analysis utilized a quartz cell containing 3.0 mL of accurately calibrated fibrinogen solution (10×10^{-6} mol/L). During titration, the TM drug solution (50×10^{-6} mol/L) was introduced incrementally. A 2.5 μL micro-syringe enabled precise injection of the drug solution into the quartz cell. Excitation wavelengths for fibrinogen started at 280 nm, and slit widths of 5 nm were used in steady-state fluorescence spectrum tests with emission wavelengths ranging from 300 to 500 nm.

Circular dichroism spectroscopy
A Jasco J-1700 spectrophotometer with a 2 mm path length and continuous nitrogen flow was used to perform CD measurements of fibrinogen both with and without TM. The study was carried out in the 250–350 nm range at a speed of 50 nm/min. To create stock solutions, 10μM fibrinogen and 10μM TM were added individually to 0.05 M buffer. To get to a final concentration of 1.25 μM, both solutions were diluted. At molar ratios of 1:3 and 1:5, fibrinogen and TM aggregates were investigated. At room temperature (25 °C), secondary complex variation analysis and protein α-helicity evaluation were carried out.

Molecular docking method
Molecular docking investigations were conducted using the Glide program within the Schrödinger software suite. The rental application was employed for the FB and TM terminals. A Van der Waals radius of 1.0 Å and default parameters were utilized in generating the receptor grid. Ligand-receptor interactions were then computed using these grids through XP ligand docking in Glide, with consideration given to the smallest hydrogen bond. The FB structure (PDB ID-4F5S) was obtained from the Protein Data Bank (PDB). The protein structure underwent optimization via Schrödinger's Protein Preparation Wizard module before docking. Preprocessing involved selecting additional bonding sequences before hydrogen addition. Heteroatoms were ionized at physiological pH to assess medication solubility and protein accessibility. The Schrödinger Ligure algorithm facilitated the conversion of 2D ligand structures to 3D. Energy minimization of the ligand structure was achieved using the OPLS3 force field. Low-energy binding complexes were utilized in the docking studies.

Result and discussion

Fluorescence investigations of FB and TM

Studies using fluorescence spectroscopy are essential for elucidating the binding interactions between medications and biomolecules. When excited at 280 nm, FB alone displays an absorption peak around 350 nm. As the concentration of the drug (TM) increases, a consistent decrease in fluorescence emission intensity is observed. Prior research indicates that these fluorescence variations correlate with the number of disulfide bonds broken after irradiation, with a reduction in disulfide bonds leading to enhanced fluorescence intensity[25]. To comprehend the fluorescence mechanism of TM-FB interactions, investigations were conducted at 290 K, 298 K, and 305 K which are shown in Figs. 2, 3 and 4. The quenching process can be explicated through Eq. (1) i.e. Stern-Volmer equation, derived from further data analysis from the graph shown in Fig. 5[26].

$$\frac{F_\circ}{F} = 1 + K_{SV}\,[Q] = 1 + K_q \tau_\circ\,[Q] \tag{1}$$

$$K_q = \frac{K_{SV}}{\tau_\circ} \tag{2}$$

Here, [Q] denotes the quencher concentration, K_q represents the FB quenching rate, the unquenched fluorophore lifespan is denoted by τ_0, while the Stern-Volmer constant is represented by K_{sv}. FB's fluorescence intensities with and without TM are represented by the letters F and F0, respectively. Equation (2) was used to determine K_q values, assuming a protein fluorescence lifetime of 10^{-8} s. A K_q value below 10^{-8} s indicates dynamic quenching, while a value exceeding 10^{-8} s suggests static quenching[27]. Elevated temperatures increase molecular mobility, enhancing dynamic collision and quenching. This results in a temperature-dependent increase in K_{sv}, characteristic of dynamic quenching[28]. Conversely, if rising temperatures destabilize initial state complex formation, K_{sv} decreases with temperature, suggesting a predominant static quenching mechanism[29]. The binding characteristics of FB-TM complexes, including the binding constant (K_b) and number of binding sites (n), were calculated based on the assumption that specific binding sites exist in FB[30].

$$\log \frac{F_\circ - F}{F} = \log K_b + n \log [C] \tag{3}$$

The binding constant, K_b, and the number of binding sites on each protein molecule, n, are included in Eq. (3). A graph in Fig. 6 was produced at three different temperatures (290 K, 298 K, and 308 K) to calculate the values of K_b and n. A linear correlation between log k and 1/T is evident from Fig. 7. The slope and intercept of this plot were used to determine ΔH and ΔS, which are reported in Table 2. Additionally, Eqs. (4) and (5) were used for the calculation of the Gibbs free energy.

$$ln K_b = -\frac{\Delta H}{RT} + \frac{\Delta S}{T} \tag{4}$$
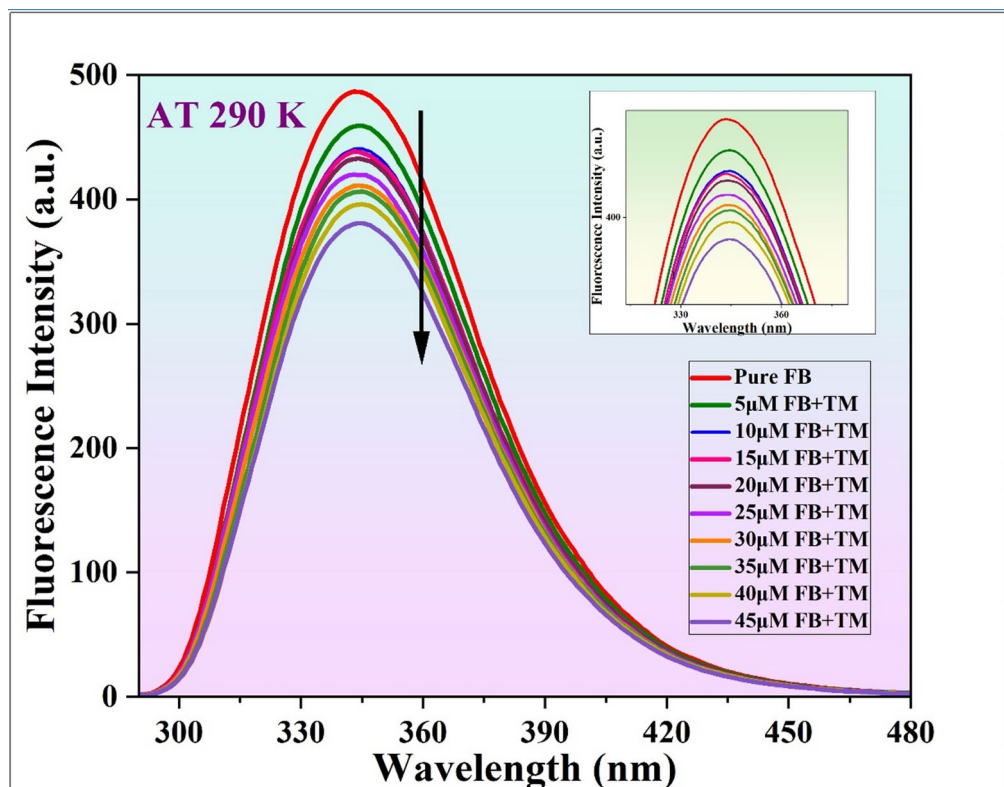
$$\Delta G = RT \ln K_b \tag{5}$$

Fig. 2. Emission spectra of FB at temperature 290 K with and without TM employing fluorescence spectroscopy.

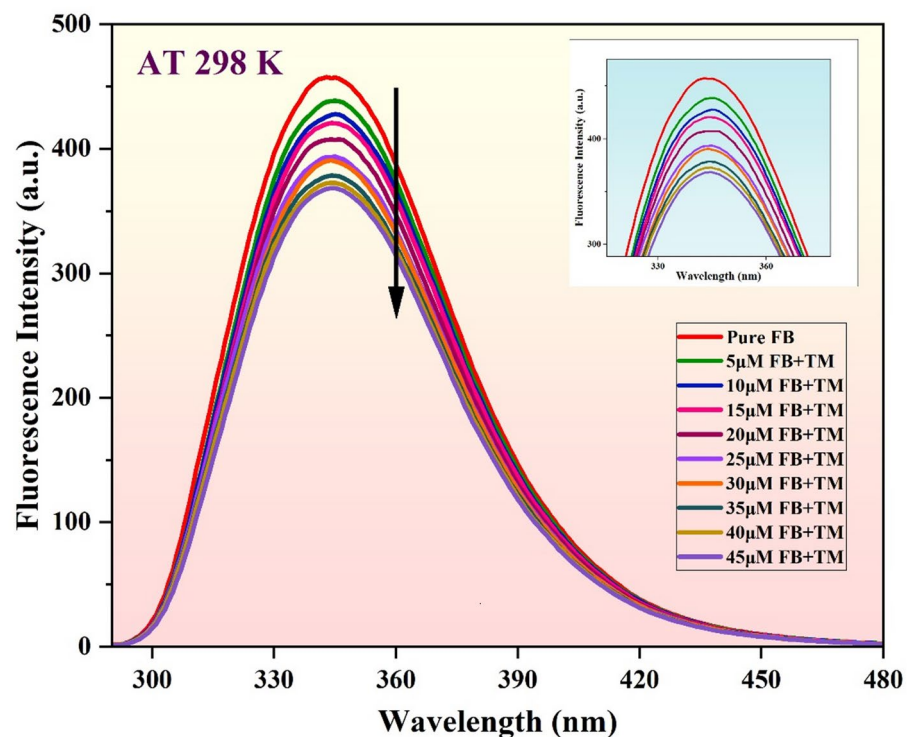**Fig. 3**. Emission spectra of FB at temperature 298 K with and without TM employing fluorescence spectroscopy.
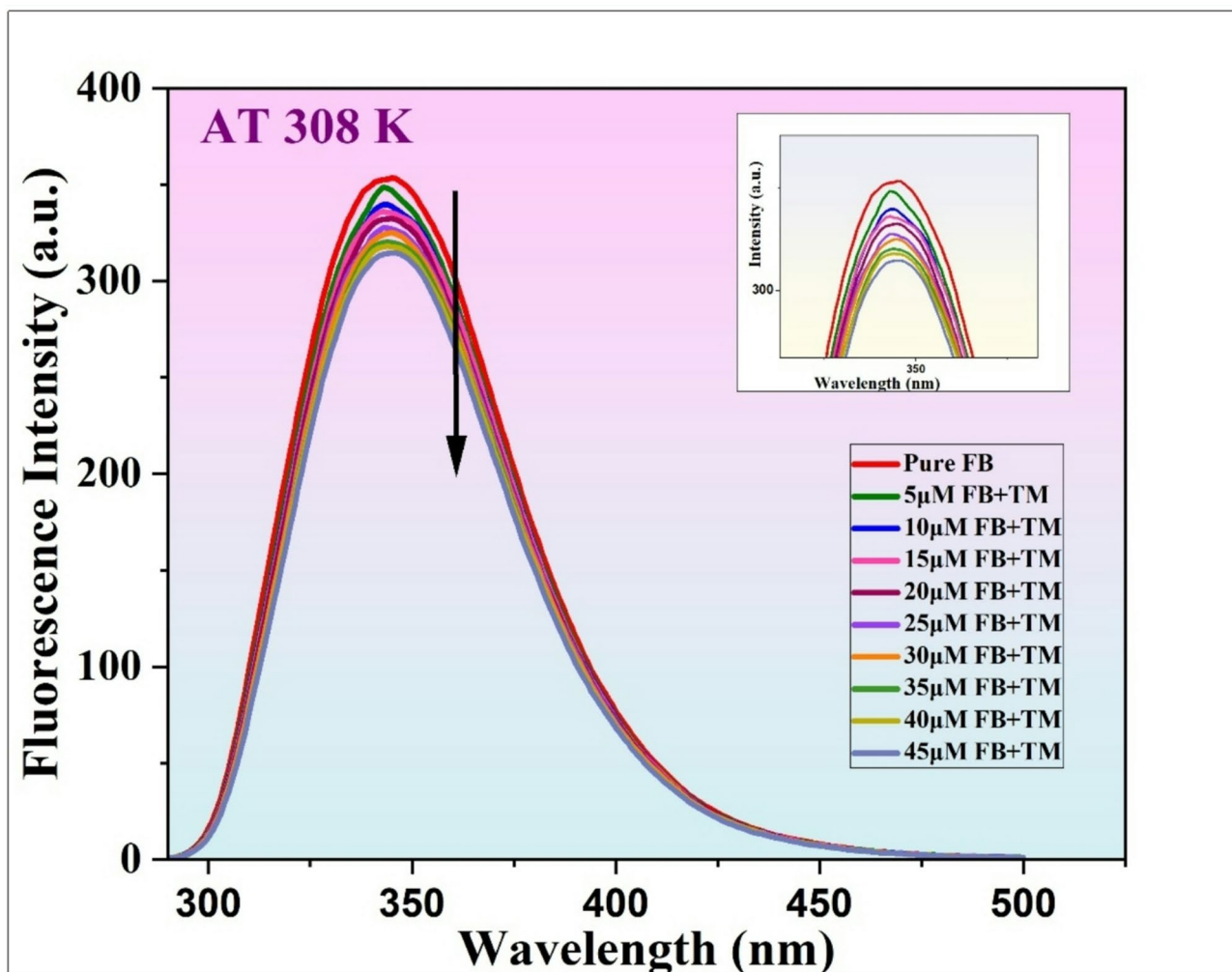
Fig. 4. Emission spectra of FB at temperature 308 K with and without TM employing fluorescence spectroscopy.

Where T is the temperature (290 K, 298 K, and 308 K), R is the gas constant (1.987 calmol$^{-1}K^{-1}$), and K_b is the binding constant. For the interaction between TM and FB, the binding parameters are shown in Tables 1 and 2. A negative value for ΔG indicates that the interaction process is spontaneous[31].

Circular dichroism investigations of FB and TM

Circular Dichroism (CD) serves as a highly sensitive spectroscopic approach for investigating protein secondary structures and examining polypeptide chain conformations during ligand binding[32]. The plasma glycoprotein FB, characterized by its substantial α-helical content, displays CD spectra with distinctive negative peaks at 208 nm and 222 nm, validating its α-helical secondary structure. Studies by Razumovsky et al. have shown that FB is composed of 42% helices, 30.8% random coils, 7% sheets, and 20% turns[33]. These spectral signals facilitate quantitative analysis to estimate α-helical content and track conformational changes when proteins interact with small molecules or external agents[34,35]. The binding of TM to FB may induce shifts in the intensity or position of the negative peaks at 208 and 222 nm, potentially signifying a gradual reduction in α-helical content. The observation of two negative bands, corresponding to the π–π* and n–π* amide transitions of the polypeptide chain, confirmed the α-helical structure of the protein[36,37]. Figure 8 illustrates two distinct bands near 208 and 216 nm, characteristic of FB's alpha-helical secondary structure.

The introduction of FB and TM at molar ratios of 1:3 and 1:5 resulted in significant changes in peak shapes and positions, indicating the onset of protein denaturation. Analysis of the FB spectra revealed a protein containing both α-helical and β-sheet components. Structural alterations are indicated by a decrease in α-helix content, from the Table 3 it was concluded that the α-helix content in native FB is 18% but when the molar concentration of TM is added to the native FB the α-helix content is decreased to 1.1% and 0.1%, as evidenced by changes in the ellipticity of negative peaks. This analysis, conducted using BESTSEL software and depicted in Fig. 9a–c, quantifies the relative proportions of these structural elements.
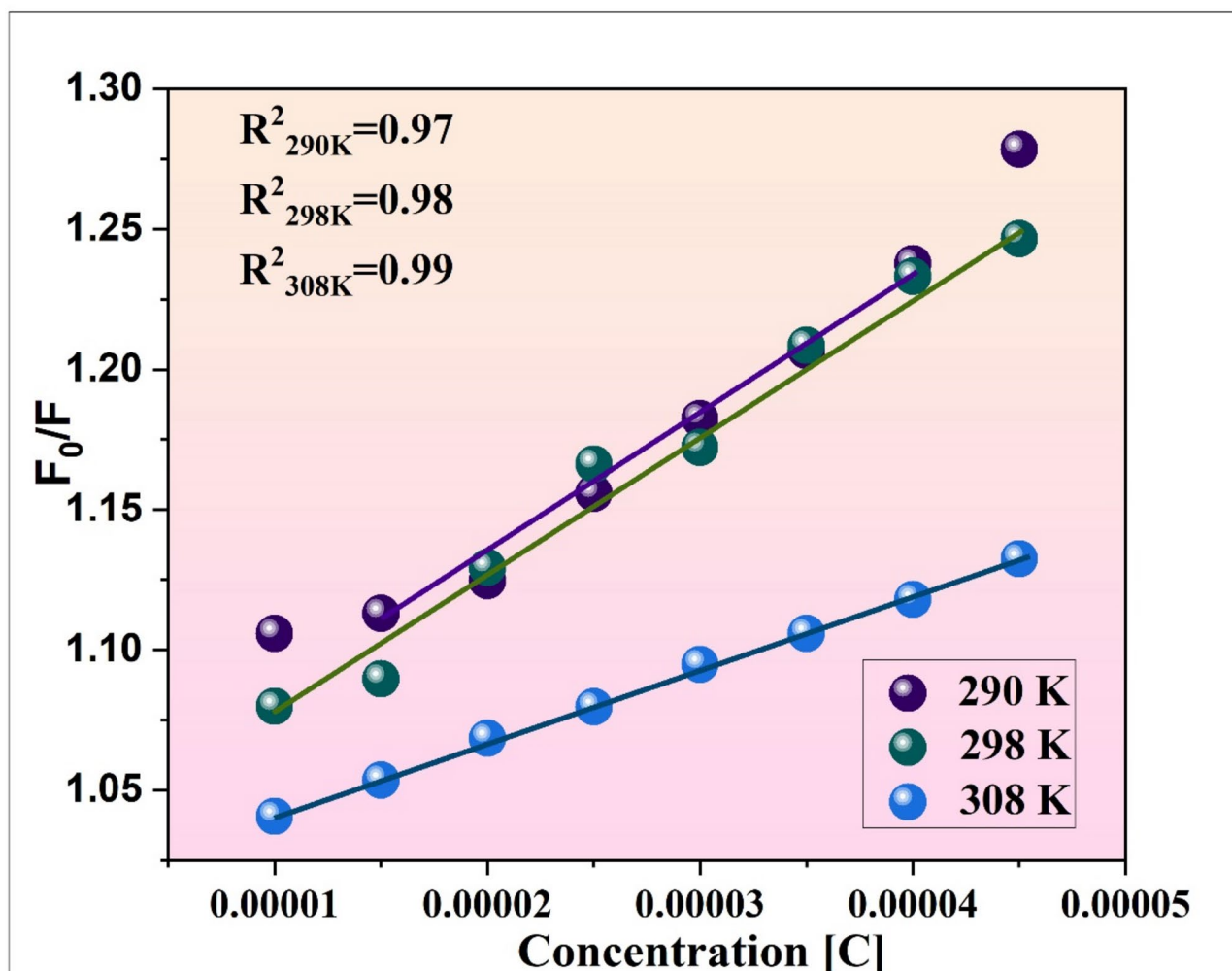
Fig. 5. The Stern–Volmer plots of fluorescence quenching spectra of FB and TM complex at three different temperatures.

Molecular Docking investigations of FB and TM

The process of pinpointing and anticipating viable binding sites within receptor protein molecules plays a crucial role in validating theoretical methodologies[38]. Molecular docking investigations offer a robust theoretical framework for elucidating complex binding mechanisms. Three primary domains make up the structure of FB: two peripheral D domains and a core E domain[39–41]. Analysis of the docking scores for TM-FB complex interactions provides crucial insights into binding dynamics. The magnitude of the docking score correlates positively with the stability of protein-ligand complexes[42,43].

Timolol, one of the two constituents in TM (timolol and maleate), exhibited superior binding properties and a higher affinity for FB. As shown in Figs. 10 and 11, Two-dimensional and Three-dimensional analyses elucidated the mechanisms through which TM interacts with FB, involving hydrophobic contacts, hydrogen bonding, and Van der Waals forces[44–47]. TM was observed to interact near the coiled (E5 region). As illustrated in Fig. 10, TM forms three hydrogen bonds with the residues SER N:50, GLY Q:51, and CYS Q:48, with bond distances of 2.36 Å, 2.35 Å, and 2.18 Å, respectively. The binding process is mediated by interactions with specific residues, including THR21, THR22, THR85, CYS19, CYS48, CYS83, GLY86, PRO20, PRO49, and PRO84. Functioning as the primary binding component of TM, timolol demonstrates an optimal active binding configuration, as evidenced by its total binding score of − 7.136 kcal/mol. These findings underscore the ionic nature of TM's strong binding capacity, which facilitates the interaction between TM and FB.

Conclusion

The study explored the FB-TM interaction at the molecular level under physiological conditions using circular dichroism, fluorescence emission, and molecular docking methods. According to experimental results, TM binding to FB caused a hypochromic shift, and TM may have quenched fibrinogen's natural Trp residues through dynamic fluorescence quenching. Stern-Volmer constants and binding constants were found to be $(5.026 \times 10^3 \, \mathrm{Lmol}^{-1}, 5.143 \times 10^3 \, \mathrm{Lmol}^{-1}, 2.465 \times 10^3 \, \mathrm{Lmol}^{-1})$ and $(1.45 \times 10^2 \, \mathrm{Lmol}^{-1}, 6.05 \times 10^2 \, \mathrm{Lmol}^{-1}, 2.798 \times 10^3 \, \mathrm{Lmol}^{-1})$ at 290 K, 298 K, and 308 K, respectively, indicating strong TM-FB interaction. Positive ΔH and ΔS
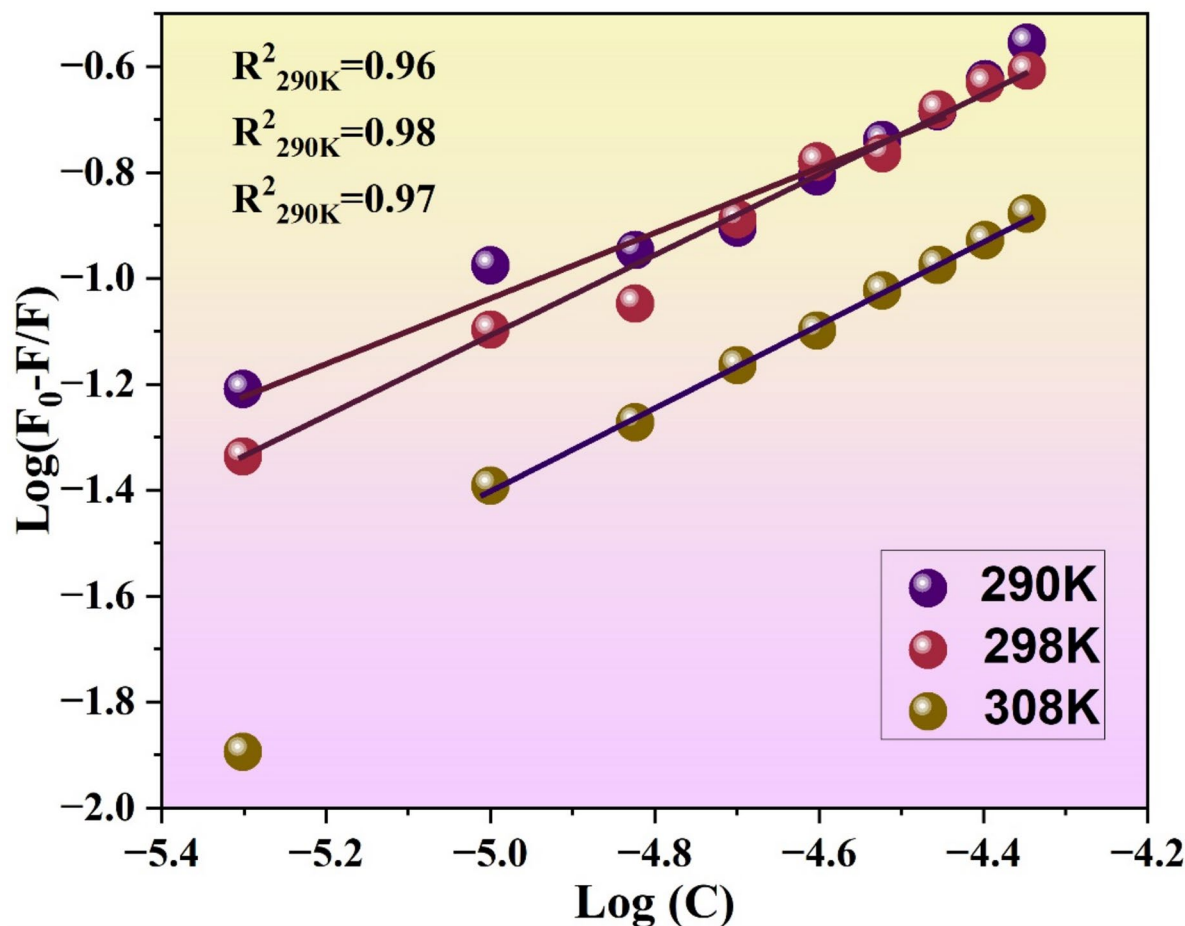
Fig. 6. The plots of $\log \frac{F_0 - F}{F}$ against Log [C] FB and TM complex at 3 different temperatures.

values further confirmed hydrophobic interactions. CD spectroscopy revealed that TM interaction decreased in α-helical content in FB's secondary structures. Thermodynamic and molecular docking analyses suggested that hydrophobic interaction as well as hydrogen bonding governs the.

TM-FB interaction, with a binding score of – 7.136 kcal/mol. By shedding light on TM's stability and interaction processes with FB, this study advances our knowledge of the crucial drug-protein interactions that underpin pharmacological effectiveness. The findings offer a deeper understanding of TM-induced changes in protein microenvironments, which can be applied to developing drugs with enhanced efficacy and improved delivery.
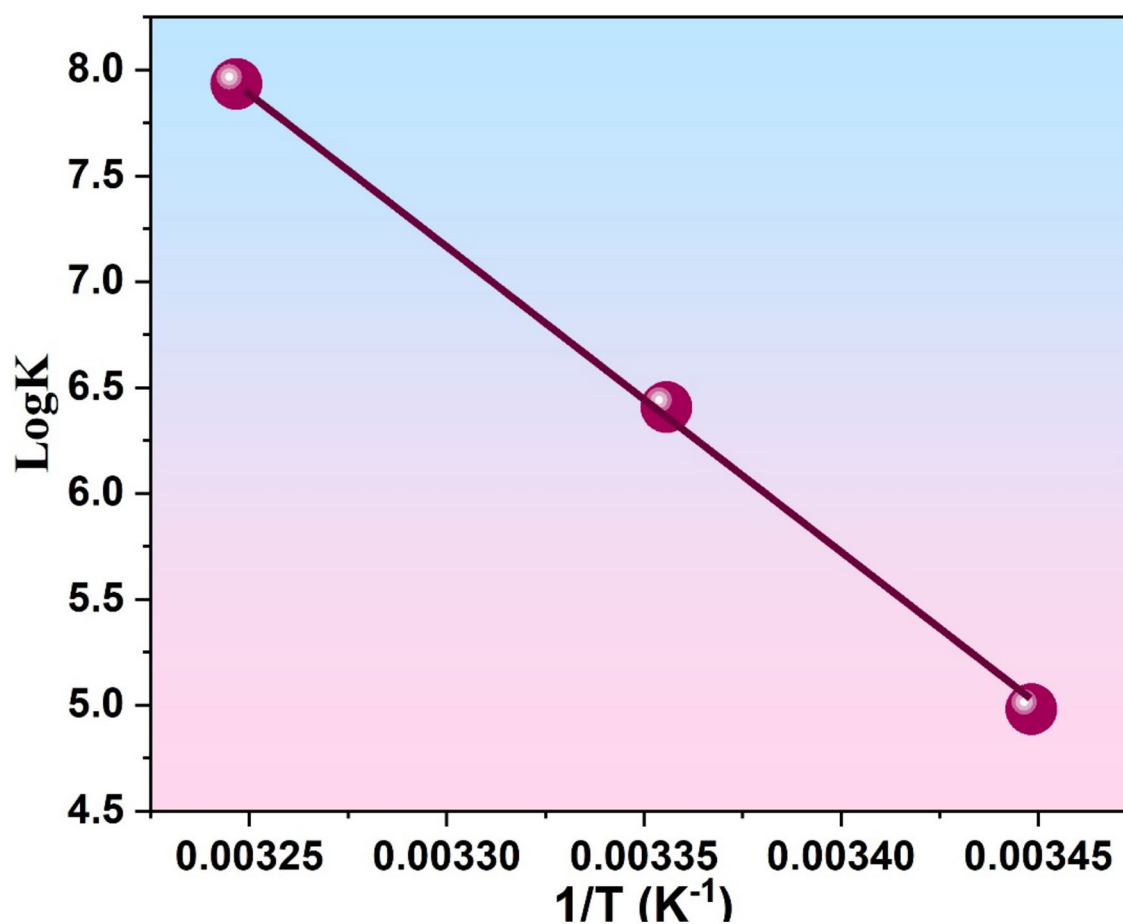
Fig. 7. Van't Hoff's plot illustrating FB and TM interaction.

Temperature	Stern-Volmer constant (K_{SV}) Lmol^{-1}	Quenching constant (K_q) Lmol^{-1} s
290 K	5.026×10^3	5.026×10^{11}
298 K	5.143×10^3	5.143×10^{11}
308 K	2.465×10^3	2.465×10^{11}

Table 1. Fluorescence spectroscopy was employed for obtaining thermodynamic parameters at temperatures of 290 K, 298 K, and 308 K.

Temperature	Binding constant (K_b) Lmol^{-1}	binding sites (n)	Gibbs's energy change (ΔG) Kcal/mol	ΔH Kcal/mol	ΔS Kcal/mol
290 K	1.45×10^2	0.6	− 6.609	66.963	253.81
298 K	6.05×10^2	0.7	− 8.736	66.963	253.81
308 K	2.798×10^3	0.9	− 11.181	66.963	253.81

Table 2. Fluorescence spectroscopy was employed for obtaining thermodynamic parameters at temperatures of 290, 298, and 308 K.
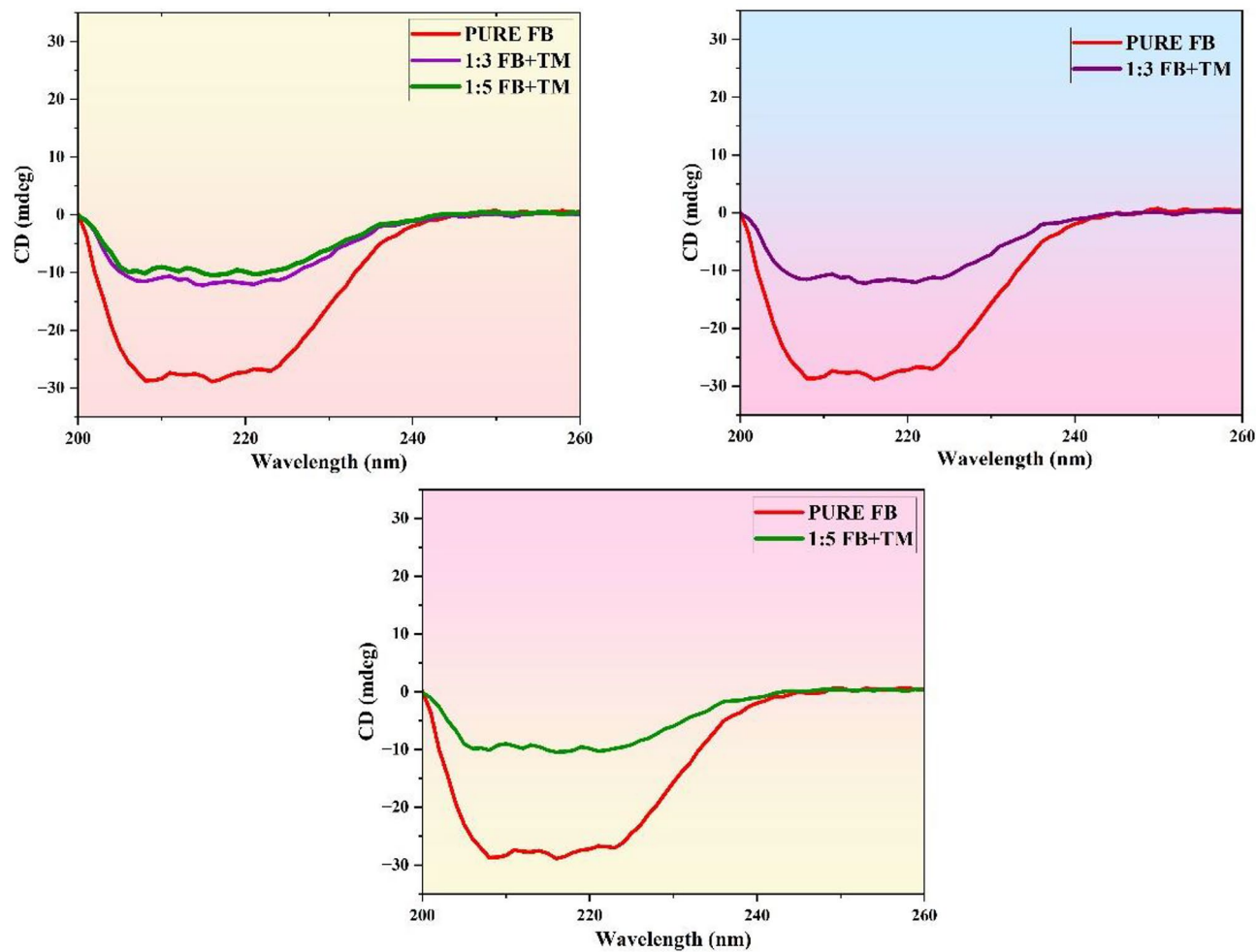
Fig. 8. CD Spectra of FB and TM at two different concentration ratios 1:3 and 1:5 at pH 8.4.

Ratio of FB: TM ratio	α-helix	
	Helix(regular)	Helix (distorted)
1:0	8.3	9.7
1:3	1.1	0.0
1:5	0.1	0.0
Ratio of FB: TM ratio	β-sheets			
	Antiparallel	Parallel	Turn	Others
1:0	18.9	2.8	15.3	45.1
1:3	39.2	0.0	13.8	45.9
1:5	38.9	0.0	14.4	46.5

Table 3. α-helical and β-sheet content at different ratios of concentration of FB and TM.

(a)

(b)

(c)
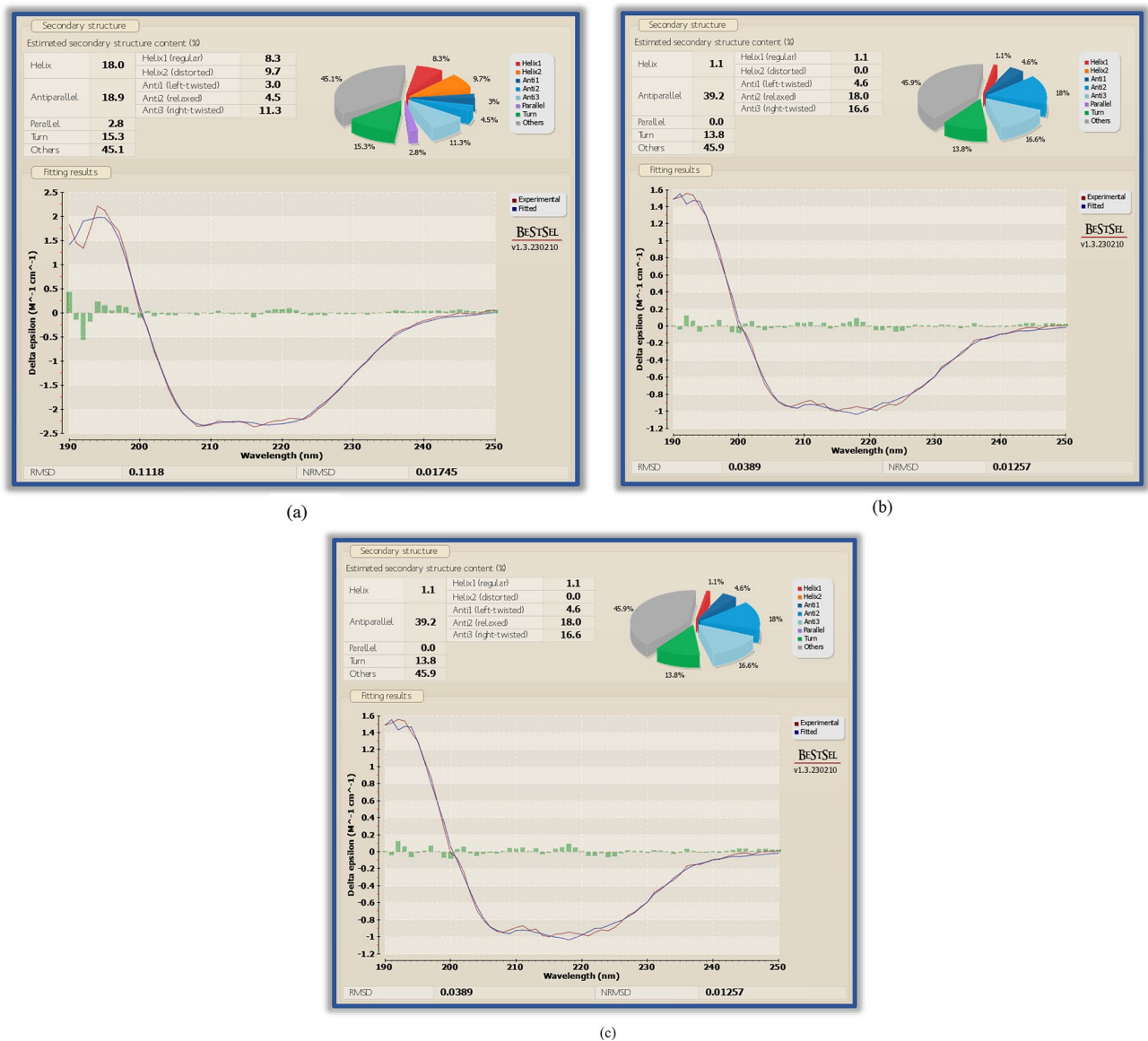
Fig. 9. (a) Results of CD spectra of pure FB at pH 8.4 using BESTSEL software. (b) Results of CD Spectra of FB and TM at concentration ratios 1:3 (pH 8.4) using BESTSEL software. (c) Results of CD Spectra of FB and TM at concentration ratios 1:5 (pH 8.4) using BESTSEL software.
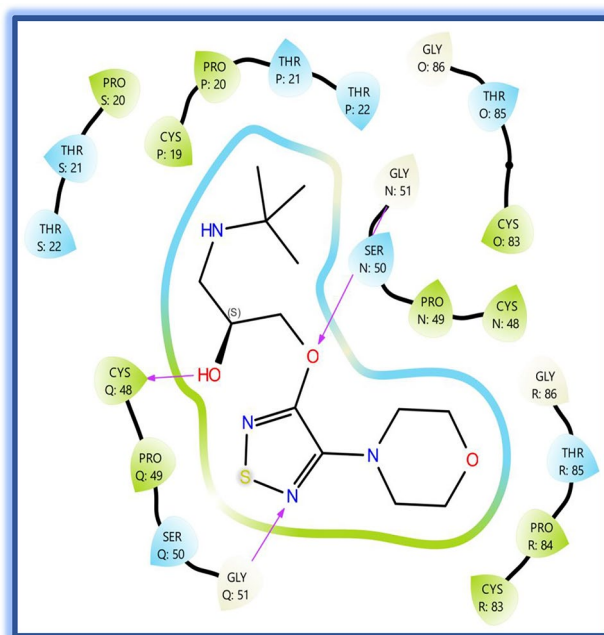
Fig. 10. 2-Dimensional Representation of FB protein in (central part) E5-region highlighting the binding sites that interact with the Timolol.
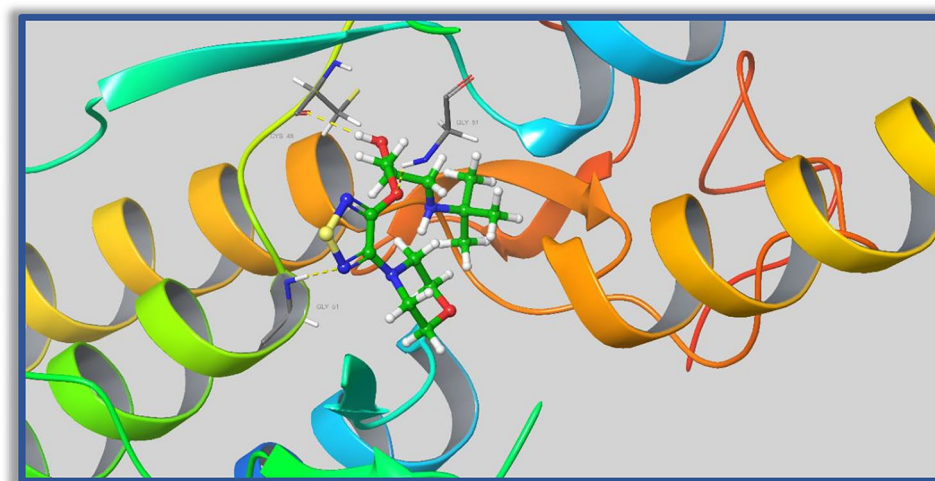

Fig. 11. 3-Dimensional Representation of FB protein in (coiled part) E5-region highlighting the binding sites that interact with the Timolol.

Data availability
The data will be available on request to the corresponding author.

References
1. Chung, D. W., Rixon, M. W., Que, B. G. & Davie, E. W. Cloning of fibrinogen genes and their cDNA. *Ann. N. Y. Acad. Sci.* **408**, 449–456 (1983).
2. Bingham, E. C. & Roepke, R. R. The rheology of the blood. II. The effect of fibrinogen on the fluidity of blood plasma. *J. Am. Chem. Soc.* **64** (5), 1204–1206 (1942).
3. Bratek-Skicki, A., Żeliszewska, P. & Ruso, J. M. Fibrinogen: a journey into biotechnology. *Soft Matter*. **12** (42), 8639–8653 (2016).
4. Cohen, C. et al. The structure of fibrinogen and fibrin: I. Electron microscopy and X-ray crystallography of fibrinogen. *Ann. NY Acad. Sci.* **408**, 194–213 (1983).

5. Zhang, H., Wu, P., Zhu, Z. & Wang, Y. Interaction of γ-Fe2O3 nanoparticles with fibrinogen. *Spectrochim. Acta Part A Mol. Biomol. Spectrosc.* **151**, 40–47 (2015).
6. De Cristofaro, R. & Di Cera, E. Modulation of thrombin-fibrinogen interaction by specific ion effects. *Biochemistry* **31** (1), 257–265 (1992).
7. Marucco, A. et al. Hydroxyl density affects the interaction of fibrinogen with silica nanoparticles at physiological concentration. *J. Colloid Interface Sci.* **419**, 86–94 (2014).
8. Roy, S. & Dasgupta, A. K. Controllable self-assembly from fibrinogen–gold (fibrinogen–Au) and thrombin–silver (thrombin–Ag) nanoparticle interaction. *FEBS Lett.* **581** (28), 5533–5542 (2007).
9. Gonzalez-Durruthy, M., Rial, R., Cordeiro, M. N. D., Liu, Z. & Ruso, J. M. Exploring the conformational binding mechanism of fibrinogen induced by interactions with penicillin β-lactam antibiotic drugs. *J. Mol. Liq.* **324**, 114667 (2021).
10. Hassan, N., Maldonado-Valderrama, J., Gunning, A. P., Morris, V. J. & Ruso, J. M. Investigating the effect of an arterial hypertension drug on the structural properties of plasma protein. *Colloids Surf. B.* **87** (2), 489–497 (2011).
11. Oliver, E., Mayor Jr, F. & D'Ocon, P. Beta-blockers: historical perspective and mechanisms of action. *Rev.Española De Cardiol. (Engl. Ed.)* **72** (10), 853–862 (2019).
12. Opie, L. H. Basis for cardiovascular therapy with beta-blocking agents. *Am. J. Cardiol.* **52** (9), D2–D9 (1983).
13. Mazzo, D. J. & Loper, A. E. Timolol maleate. In *Analytical Profiles of Drug Substances, Vol. 16* 641–692 (Academic, 1987).
14. Karhuvaara, S., Kaila, T. & Huupponen, R. β-Adrenoceptor antagonist activities and binding affinities of timolol enantiomers in rat atria. *J. Pharm. Pharmacol.* **41** (9), 649–650 (1989).
15. Volotinen, M., Hakkola, J., Pelkonen, O., Vapaatalo, H. & Mäenpää, J. Metabolism of ophthalmic Timolol: new aspects of an old drug. *Basic Clin. Pharmacol. Toxicol.* **108** (5), 297–303 (2011).
16. Nino, J. et al. Cardiovascular effects of ophthalmic 0.5% timolol aqueous solution and 0.1% timolol hydrogel. *Clin. Physiol. Funct. Imaging* **22** (4), 271–278 (2002).
17. Sweany, A. E., Moncloa, F., Vickers, F. F. & Zupkis, R. V. Antiarrhythmic effects of intravenous timolol in supraventricular arrhythmias. *Clin. Pharmacol. Ther.* **37** (2), 124–127 (1985).
18. Lazreg, S. et al. Efficacy and safety of preservative-free timolol 0.1% gel in open-angle glaucoma and ocular hypertension in treatment-naïve patients and patients intolerant to other hypotensive medications. *J. Fr. Ophtalmol.* **41** (10), 945–954 (2018).
19. Kandagal, P. B., Seetharamappa, J., Shaikh, S. M. T. & Manjunatha, D. H. Binding of Trazodone hydrochloride with human serum albumin: a spectroscopic study. *J. Photochem. Photobiol. A* **185** (2–3), 239–244 (2007).
20. Jiang, Y. L. Design, synthesis and spectroscopic studies of Resveratrol aliphatic acid ligands of human serum albumin. *Bioorg. Med. Chem.* **16** (12), 6406–6414 (2008).
21. Epps, D. E., Raub, T. J., Caiolfa, V., Chiari, A. & Zamai, M. Determination of the affinity of drugs toward serum albumin by measurement of the quenching of the intrinsic Tryptophan fluorescence of the protein. *J. Pharm. Pharmacol.* **51** (1), 41–48 (1999).
22. Martinez-Landeira, P., Ruso, J. M., Prieto, G., Sarmiento, F. & Jones, M. N. The interaction of human serum albumin with Dioctanoylphosphatidylcholine in aqueous solutions. *Langmuir* **18** (8), 3300–3305 (2002).
23. Zhang, Q., Huang, Y., Zhao, R., Liu, G. & Chen, Y. Determining binding sites of drugs on human serum albumin using FIA-QCM. *Biosens. Bioelectron.* **24** (1), 48–54 (2008).
24. Mandeville, J. S., Froehlich, E. & Tajmir-Riahi, H. A. Study of Curcumin and genistein interactions with human serum albumin. *J. Pharm. Biomed. Anal.* **49** (2), 468–474 (2009).
25. Renner, S., Derksen, S., Radestock, S. & Mörchen, F. Maximum common binding modes (MCBM): consensus Docking scoring using multiple ligand information and interaction fingerprints. *J. Chem. Inf. Model.* **48** (2), 319–332 (2008).
26. Khatun, S. Riyazuddeen, interaction of Colchicine with BSA: spectroscopic, calorimetric and molecular modelling approaches. *J. Biomol. Struct. Dyn.* **36** (12), 3122–3129 (2018).
27. Ling, X., Zhong, W., Huang, Q. & Ni, K. Spectroscopic studies on the interaction of Pazufloxacin with calf thymus DNA. *J. Photochem. Photobiol., B* **93** (3), 172–176 (2008).
28. Ameen, F. et al. A detailed insight into the interaction of memantine with bovine serum albumin: a spectroscopic and computational approach. *J. Mol. Liq.* **303**, 112671 (2020).
29. Shahabadi, N. & Amiri, S. Spectroscopic and computational studies on the interaction of DNA with Pregabalin drug. *Spectrochim. Acta Part A Mol. Biomol. Spectrosc.* **138**, 840–845 (2015).
30. Fu, L. et al. Mechanism evaluation of the interactions between flavonoids and bovine serum albumin basedonmulti-spectroscopy, molecular docking and Q-TOFHR-MS analyses. *Food Chem.* **203**, 150–157 (2016).
31. Saranya, V., Mary, P. V., Vijayakumar, S. & Shankar, R. The hazardous effects of the environmental toxic gases on amyloid betapeptide aggregation: a theoretical perspective. *Biophys. Chem.* **263**, 106394 (2020).
32. Woody, R. W. Circular dichroism. *Methods Enzymol.* **246**, 34–71 (1995).
33. Alamdari, S. et al. Orientation and conformation of proteins at the air–water interface determined from integrative molecular dynamics simulations and sum frequency generation spectroscopy. *Langmuir* **36** (40), 11855–11865 (2020).
34. Ahmad, E. et al. Stereo-selectivity of human serum albumin to enantiomeric and isoelectronic pollutants dissected by spectroscopy, calorimetry and bioinformatics. *Plos One* **6** (11), e26186 (2011).
35. Bonechi, C., Martini, S. & Rossi, C. Interaction study of bioactive molecules with fibrinogen and human platelets determined by 1H NMR relaxation experiments. *Bioorg. Med. Chem.* **17**, 1630–1635 (2009).
36. Azpiazu, I. & Chapman, D. Spectroscopic studies of fibrinogen and its plasmin-derived fragment. *Biochim. Biophys. Acta* **1119** (3), 268–274 (1992).
37. Barbucci, R., Lamponi, S. & Magnani, A. Fibrinogen conformation and platelet reactivity in relation to material–blood interaction: effect of stress hormones. *Biomacromolecules* **4**, 1506–1513 (2003).
38. Ahmad, E., Rabbani, G., Zaidi, N., Ahmad, B. & Khan, R. H. Pollutant-induced modulation in conformation and β-lactamase activity of human serum albumin. *PLoS One* **7**(6), e38372 (2012).
39. Madrazo, J. et al. Crystal structure of the central region of bovine fibrinogen (E5 fragment) at 1.4-Å resolution. *Proc. Natl. Acad. Sci.* **98**(21), 11967–11972 (2001).
40. Kollman, J. M., Pandi, L., Sawaya, M. R., Riley, M. & Doolittle, R. F. Crystal structure of human fibrinogen. *Biochemistry* **48** (18), 3877–3886 (2009).
41. Pechik, I., Yakovlev, S., Mosesson, M. W., Gilliland, G. L. & Medved, L. Structural basis for sequential cleavage of fibrinopeptides upon fibrin assembly. *Biochemistry* **45** (11), 3588–3597 (2006).
42. Weisel, J. W., Phillips, G. N. Jr & Cohen, C. The structure of fibrinogen and fibrin: II. Architecture of the fibrin clot. *Ann. N. Y. Acad. Sci.* **408**, 367–379 (1983).
43. Syahbanu, F., Giriwono, P. E., Tjandrawinata, R. R. & Suhartono, M. T. Molecular Docking of subtilisin K2, a fibrin-degrading enzyme from Indonesian Moromi, with its substrates. *Food Sci. Technol.* **42**, e61820 (2021).
44. Li, X., Duan, H., Song, Z. & Xu, R. Comparative study on the interaction between fibrinogen and flavonoids. *J. Mol. Struct.* **1262**, 132963 (2022).
45. González-Durruthy, M. et al. Targeting beta-blocker drug–drug interactions with fibrinogen blood plasma protein: a computational and experimental study. *Molecules* **25** (22), 5425 (2020).
46. Aalikhani, M., Alikhani, M., Shamsabadi, F., Oladnabi, M. & Bazi, Z. In Silico drug repurposing for the treatment of heart diseases using gene expression data and molecular Docking techniques. *Biochem. Biophys. Res. Commun.* **572**, 138–144 (2021).

47. González-Durruthy, M., Rial, R., Liu, Z. & Ruso, J. M. Lysozyme allosteric interactions with β-blocker drugs. *J. Mol. Liq.* **366**, 120370 (2022).

Acknowledgements

Author contributions

Neha Govind Rao: Writing, conceptualizationAnu Radha Pathania: Data analysis, Figure preparationHarman Deep Kour: Investigation, writingSuhas Ballal: Methodology, SupervisionAbhayveer Singh: Graph preparation, Review writingAbhijit Bhowmik: Data analysis, Review writingBalewgize A. Zeru: Supervision, Funding.

Competing interests

The authors declare no competing interests.

Human and animal rights

The research's basic investigations did not involve the use of humans or animals.

Additional information

Correspondence and requests for materials should be addressed to B.A.Z.

Reprints and permissions information is available at www.nature.com/reprints.

Publisher's note Springer Nature remains neutral with regard to jurisdictional claims in published maps and institutional affiliations.